J Mater Sci: Mater Electron (2016) 27:13034–13043
DOI 10.1007/s10854-016-5444-y

Change of mechanical performance and characterization with replacement of Ca by Gd nanoparticles in Bi-2212 system and suppression of durable tetragonal phase by Gd

Bahadir Akkurt[1] · Gurcan Yildirim[1]

Received: 3 July 2016 / Accepted: 25 July 2016 / Published online: 27 July 2016
© Springer Science+Business Media New York 2016

Abstract In this study, we concentrate on crucial evaluations of mechanical performances belonging to $Bi_{2.1}Sr_{2.0}Ca_{1.1-x}Gd_xCu_{2.0}O_y$ superconducting ceramics with the partial replacement within the molar ratio change $0 \leq x \leq 0.30$ of aliovalent Gd-sites on the Ca-sites in the system by means of microhardness measurements at different static compression test loads in the range of 0.245–2.940 N. The experimental measurement findings observed display that the mechanical performance tends to regress regularly with the enhancement of the Gd content level due to the increment in the local structural distortions, boundary weak connection between the grains and lattice disorders/strains/defects in the orientation of superconducting adjacent layers. Namely, the presence of Gd foreign impurities in the Bi-2212 crystal lattice leads to induce the crack-producing omnipresent flaws acting as the stress raisers and crack initiation sites. The long and short of it is that the Ca/Gd substitution in the adjacent layers damages seriously the mechanical strength (durability and stiffness), fracture and flexural strengths of the Bi-2212 material due to the increased operable slip systems so that the intergranular fracture becomes more dominant in the Bi-2212 matrix. In other words, the increment in Gd substitution level at the Ca site leads to accelerate the crack propagation and dislocation movement as a result of the decrement in Griffith critical crack length. Thus, the critical stress and durable tetragonal phase values degrade considerably in parallel to the enhancement of Gd content level, and the augmented cracks and dislocations with the existence of foreign impurities reach instantly to the critical propagation speed. The propagation of cracks and dislocation movements is hard to control along with the superconducting samples. At the same time, the Gd inclusions lead to change in mechanical characterization of the Bi-2212 ceramics. The pure sample presents Indentation Size Effect (*ISE*) behavior while the others exhibit Reverse Indentation Size Effect (*RISE*) feature, pointing out the increment of induced structural distortions and grain boundary couplings. Besides, the Vickers hardness experimental results are analyzed by the offered theoretical model of Hays–Kendall approach for the first time.

1 Introduction

Hardness means the resistance of materials to be immersed in a hard pointed end [1]. Generally, a standard pointed end is strongly suppressed to object with a fixed test load in the experimental measurements, thus the magnitudes formed by the sinking are considered as a measurement of the resistance to plastic (permanent) deformation of the material [2]. The hardness is also provided by means of surface scratch or indentation with impact and bounce back of launched body except indentation with applying a static test force [2, 3]. The values of hardness just compare the numbers due to the fact that the resulting values are not used directly in the design. However, the scientists have widely used the hardness techniques in the quality control because of the easy application of method [4–9]. It is another advantage to provide information about the strength and abrasion behavior of the material by leaving only a small footprint.

At the same time, the hardness identification tests can be used for materials exhibiting different hardness and

✉ Bahadir Akkurt
bahadirakkurt@ibu.edu.tr

[1] Department of Mechanical Engineering, Abant Izzet Baysal University, 14280 Bolu, Turkey

thickness, namely, they take first place as the mechanical characterization method in large application areas. It is possible to determine the hardness of different regions in the working material microstructure by using very little force and the microscope. Selection of the most appropriate methods among different hardness methods plays an important role in understanding the hardness of bulk metals, composites and ceramic materials. The most common indentation hardness scales used for the hardness of metals and alloys are: Brinell, Rockwell, Knoop and Vickers hardness techniques [10, 11]. In superconductivity, the Vickers hardness is most preferable due to their own superiority such as nondestructive nature, easy test procedure, quite low cost, accurate reading and especially independent of indentation test load exerted on the measured hardness test [12, 13]. It is another advantage of Vickers hardness technique that the specimen surfaces are rarely damaged during the test. In this respect, the measurement findings deduced from the microhardness method are reliable and useful for the quality control treatments and material selections in the metallurgical, engineering, technological and industrial applications. However, the slight increment in the elasticity (the hardness parameters are found to be slightly higher than they should be) leads to appear a negative property along with the Vickers hardness test.

In the current work, the important changes of mechanical performances (stiffness, durability, fracture and flexural strength) and characterizations (*ISE* or *RISE* behavior) belonging to the inorganic Bi-2212 ceramic compounds are seriously determined by means of microhardness measurements performed at five different applied static test loads between 0.245 and 2.940 N. Moreover, the experimental curves enable us to define the critical propagation speeds, Griffith critical lengths, critical stress values and durable tetragonal phases. Additionally, the effects of Gd inclusions in the Bi-2212 crystal core on the load dependent mechanical properties regarding elastic moduli, yield strengths, fracture toughness, brittleness indices and stiffness coefficients are described in detail. Furthermore, the variation of mechanical properties is also studied by means of the theoretical model of Hays–Kendall approach and the load independent parameters are also surveyed in the plateau limit regions.

2 Preparation of materials and experimental measurements

The inorganic ceramic materials studied in this work are prepared by the standard solid-state reaction route with an initial stoichiometry of $Bi_{2.1}Sr_{2.0}Ca_{1.1-x}Gd_xCu_{2.0}O_y$ ($0 \leq x \leq 0.30$) with the use of high-purity starting oxide and carbonate powders of Bi_2O_3, $SrCO_3$, $CaCO_3$, CuO and Gd_2O_3 (commercially purchased from Alfa Aesar Co., Ltd with the purity of 99.99 %) in the medium of air. All the precursor chemical powders are accurately weighed in stoichiometric proportion by the electronic balance in the atmospheric pressure. The chemical powders weighed are milled to shrink the particle sizes in the agate mortar for half an hour by means of the pestle without any solvent/solution. First, the powders is grounded in the grinder for 8 h in the air atmosphere for the homogeneity of chemicals. The homogeneous mixture is calcinated in the three-zone programmable (Protherm-Model PTF12/75/200) furnace at the constant temperature of 800 °C for the duration of 24 h with the heating and cooling rate of 5 °C/min for the elimination of the carbon or carbon-based residuals. The resultant powder calcined is observed to turn to blackish color. Next, the blackish powder is regrounded in the agate mortar with a pestle in the absence of any solvent so that the final form of resultant powder reaches to the maximum in homogeneity. Then, the homogeneous mixture is pelletized into a rectangular bar with the volume of $20 \times 5 \times 5$ mm^3 (height of 5 mm, length of 20 mm and width of 5 mm) at the constant pressure of 300 MPa at the room temperature in the air atmosphere. The materials solidified in blackish color undergo the sintering process at the optimum temperature value of 840 °C for the duration of 36 h in the Protherm-Model furnace using the same rate of heating and cooling processes. The materials produced with different Ca/Gd partial replacement ratios of 0, 0.01, 0.03, 0.05, 0.07, 0.10 and 0.30 will hereafter be presented as Gd-0, Gd-1, Gd2, Gd-3, Gd-4, Gd-5 and Gd-6, respectively.

Both the mechanical performance and characterization studies of the inorganic $Bi_{2.1}Sr_{2.0}Ca_{1.1-x}Gd_xCu_{2.0}O_y$ samples are exerted by Vickers hardness measurements with the aid of the SHIMADZU HVM-2 model digital microhardness tester at the room temperature in the atmospheric air. The small bars are broken off from the bulk Bi-2212 materials prepared and fitted vertically into the digital indenter to achieve good experimental measurements. The static compression loads in the range from 0.245 to 2.940 N are applied on the uniform materials for the loading duration of 10 s. The two impression diagonals observed on the sample surface are detected by the calibrated microscope. The experimental measurements are conducted at different locations on the specimen surface, in case we cannot observe the extra additional in the indentation track values as a result of the surface effects and work hardening. The average values of tracks are determined from the measurements performed 8 times with the accuracy about ± 0.08 μm. All the experimental evidences enable us to easily determine the effect of Gd inclusions on the mechanical performance of the Bi-2212 superconducting

texturing. Similarly, the other mechanical parameters regarding the elastic modulus (resistance towards to plastic deformation), yield strength (beginning point of permanent plastic deformation), fracture toughness (resistant against the beginning of permanent distortion/strain), elastic stiffness coefficient (resistant towards permanent plastic deformation or strain) and brittleness index (ductility or corrosion rate) are also defined for the poly-crystallized pure and Ca/Gd substituted Bi-2212 superconducting ceramics [14, 15].

Moreover, the extracted curves from the Vickers hardness tests (change of microhardness parameters over the applied indentation test loads) allow us to discuss the mechanical characteristics of the Gd free and Ca/Gd substituted materials. As well known, there are two main mechanical characteristics for the materials as regards (I) typical indentation size effect (*ISE*) and (II) unusual reverse indentation size effect (*RISE*). The former feature is related to the non-linear decrement in load independent Vickers hardness (H_v) parameters whereas the latter behavior is associated with the enhancement in the original microhardness parameters with the increase of the static compression test loads [16–19]. The main difference between the mechanical identification stems from the surface energy values (to be discussed in the following parts) [20].

Throughout the present work, the experimental measurement findings at the saturation region are also examined by the Hays–Kendall (*HK*) model to explain the change of mechanical characterization belonging to the superconducting materials prepared in this work.

3 Results and discussion

Throughout the present work, we display the crucial changes in mechanical performance and characterization with the cationic substitution of divalent Ca^{+2} by trivalent cation Gd^{+3} in the active adjacent layers of Bi-2212 system with the aid of microhardness tests performed at the static compression loads between 0.245 and 2.940 N. All the experimental measurement results obtained are discussed in four parts. In the first part, the mechanical performance of the materials increases or decreases with the enhancement of Gd foreign impurities inserted in the Bi-2212 crystal texturing by describing the relationship between deformations (disorders, strains, defects and distortions) and mechanical performance (stiffness, durability, fracture and flexural strength). In other words, we clarify the variation of the crack propagation and dislocation movement with the presence of Gd nanoparticles in the system. Secondly, we will express the role of Gd inclusions on the mechanical characteristic behaviors (known as typical indentation size effect and unusual reverse indentation size effect) belonging to the pure Bi-2212 and Ca-site Gd substituted Bi-2212 superconducting ceramics under the static indentation test loads. In the third part, we will explain how the aliovalent Ca/Gd replacement in the Bi-2212 crystal texturing affects the load dependent characteristic parameters (elastic modulus, fracture toughness, yield strength, brittleness index and elastic stiffness coefficient) inferred from the microhardness curves. As for the last part, we determine the load independent mechanical properties in the plateau region by using the microhardness tests, and also compare the original mechanical characteristics with the available theoretical method of Hays–Kendall approach to describe the mechanical characterization of pure and Ca-site Gd substituted ceramics.

3.1 Vickers hardness experimental results

In our research for this paper, the microhardness measurements enable us to declare the effect of Gd impurities on the mechanical performance and characterization of Bi-2212 samples prepared by solid-state reaction method. As well known, the Bi-2212 material being from the Bi-based type-II superconducting parents is achieved as hard ceramics, and obtains many tiny cracks, voids and dislocations in the $Cu–O_2$ consecutively stacked sheets, leading to brittle nature [21]. In the present study, we endeavor to overcome the poor feature by doping the Gd foreign impurities in the crystal lattice for the engineering, technological and industrial application areas of the materials.

3.1.1 Change of mechanical performance with Gd inclusions

As previously mentioned in Sect. 3 of the paper, we firstly discuss the change in both the mechanical performance and durable tetragonal phase of the Bi-2212 materials with the Gd nanoparticles embedded in the crystal core. Figure 1 provides the relationship between the Vickers hardness parameters and applied indentation test loads ($0.245 \leq F_{load} \leq 2.940$ N) for the pure and Ca/Gd partially substituted Bi-2212 superconducting samples. It is apparent from the figure that the mechanical performance tends to degrade continuously with the increment of Gd content level in the superconducting matrix as a consequence of the rapid enhancement in the local structural distortions, lattice strains/defects and grain boundary coupling problems in the active adjacent layers of Bi-2212 system. In more detail, the existence of Gd inclusions in the Bi-2212 crystal texturing results in the reduction of both the critical stress value and durable tetragonal phase. This is attributed to the fact that the propagation of the induced artificial cracks, voids (stemmed from the crack initiating flaws) and dislocation movements locates in approximately

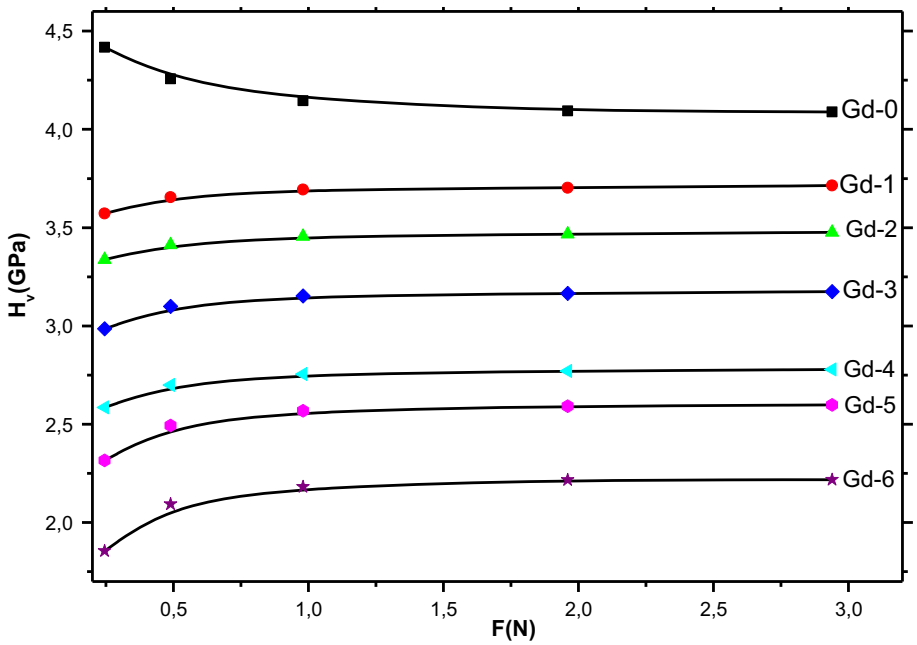

Fig. 1 Variation of Vickers hardness parameters of the pure and Ca/Gd substituted Bi-2212 ceramic materials against applied static test loads

the critical speed value due to the decrement of Griffith critical crack length. Thus, it is difficult to control the propagation of crack/void and dislocation movements due to the enhancement in the growth of initial crack. The propagations begin to proceed along with the intergranular regions (grain boundaries), and the material is broken easily. Shortly, the Gd foreign impurities inserted in the Bi-2212 superconducting system not only augment considerably the omnipresent flaws acting as the stress raisers and crack initiation sites along with the system, but also make the induced artificial cracks, voids and dislocation movements dwell in the critical propagation speed.

Likewise, the figure expresses that the mechanical strength (durability and stiffness), fracture and flexural strengths of the Ca-site Gd substituted polycrystalline $Bi_{2.1}Sr_{2.0}Ca_{1.1-x}Gd_xCu_{2.0}O_y$ ceramics retrograde systematically with the increment in the Gd concentration level up to the value of $x = 0.30$ due to the regression of durable tetragonal phase in the Bi-2212 crystal lattice. Throughout the experimental curves (microhardness parameter, H_v versus the static test loads, F_{load}), the former parameters are calculated at the different applied test loads by means of the following formula:

$$H_V = 1854.4\left(\frac{F_{load}}{d^2}\right) \quad (1)$$

where F_{load} presents the constant load applied when the abbreviation of d displays the reasonable mean impression length. Now, it is better to discuss the numerical microhardness parameters for understanding the effect of Gd foreign impurities on the mechanical performance of the inorganic compounds. One can observe all the numerical H_v values belonging to the materials in Table 1. According to the table, it is fair to conclude that the H_v values decrease constantly with the increase of the Gd concentration level in the Bi-2212 superconducting matrix at the constant indentation test load applied. To illustrate, the H_v parameters are obtained to be in a range of 4.417 GPa and 1.856 GPa at the F_{load} of 0.245 N. The maximum value is attributed to the pristine material whereas the minimum value is noted for the bulk Gd-6 sample. The similar evidences can be observed for the Vickers hardness values deduced from the other applied test loads. The dramatic decrement in the H_v values with the increment of the Gd concentration level results from new induced local structural distortions, lattice strains/disorders/defects in the Cu–O_2 consecutively stacked layers and especially the damage of boundary weak-connections between the superconducting grains. Thus, it should strongly be mentioned here that the induced artificial cracks, voids and dislocation movements reach to the critical propagation speed easily with the increment of Gd content strengthening the appearance of stress raisers and crack initiation sites in the Bi-2212 crystal structure.

At the same time, the reduction of the microhardness parameters confirms the degradation in mechanical sensitivity of the polycrystalline Bi-2212 compounds with the Gd additives inserted in the crystal lattice. Accordingly, the required test load leading to propagate the cracks and dislocations decreases considerably with the enhancement in the Gd concentration level. In this respect, the distributions of irregular grain orientation in the bulk Gd-6

Table 1 Variation of load dependent microhardness parameters such as elastic modulus (E), fracture toughness (K_{IC}), yield strength (Y), elastic stiffness coefficient (C_{11}) and brittleness index (B) as a function of applied indentation test loads for the pure and Ca/Gd substituted bulk Bi-2212 compounds

Samples	F (N)	H_v (GPa)	E (GPa)	Y (GPa)	K_{IC} (kPam$^{1/2}$)	C_{11} (GPa)	B (m$^{-1/2}$)
Gd-0	0.245	4.417	362.033	1.472	1.299	13.458	3.401
	0.490	4.257	348.919	1.419	1.275	12.616	3.338
	0.980	4.145	339.739	1.382	1.258	12.041	3.294
	1.960	4.094	335.559	1.365	1.250	11.783	3.274
	2.940	4.089	335.149	1.363	1.250	11.758	3.272
Gd-1	0.245	3.572	292.774	1.191	0.777	9.281	4.600
	0.490	3.655	299.577	1.218	0.786	9.662	4.653
	0.980	3.694	302.773	1.231	0.790	9.843	4.677
	1.960	3.703	303.511	1.234	0.791	9.885	4.683
	2.940	3.714	304.412	1.238	0.792	9.936	4.690
Gd-2	0.245	3.338	273.594	1.113	0.765	8.243	4.362
	0.490	3.413	279.741	1.138	0.774	8.570	4.411
	0.980	3.456	283.266	1.152	0.779	8.760	4.439
	1.960	3.467	284.167	1.156	0.780	8.809	4.446
	2.940	3.476	284.905	1.159	0.781	8.849	4.452
Gd-3	0.245	2.985	244.661	0.995	0.848	6.779	3.520
	0.490	3.100	254.087	1.033	0.864	7.242	3.587
	0.980	3.153	258.431	1.051	0.872	7.460	3.617
	1.960	3.166	259.496	1.055	0.873	7.514	3.625
	2.940	3.174	260.152	1.058	0.875	7.548	3.629
Gd-4	0.245	2.585	211.876	0.862	0.834	5.270	3.101
	0.490	2.700	221.301	0.900	0.852	5.687	3.169
	0.980	2.755	225.809	0.918	0.861	5.891	3.201
	1.960	2.771	227.121	0.924	0.863	5.951	3.210
	2.940	2.778	227.695	0.926	0.864	5.978	3.215
Gd-5	0.245	2.316	189.827	0.772	0.968	4.348	2.392
	0.490	2.494	204.417	0.831	1.005	4.950	2.482
	0.980	2.569	210.564	0.856	1.020	5.213	2.519
	1.960	2.592	212.449	0.864	1.024	5.295	2.530
	2.940	2.598	212.941	0.866	1.026	5.316	2.533
Gd-6	0.245	1.856	152.124	0.619	1.032	2.951	1.799
	0.490	2.094	171.632	0.698	1.096	3.645	1.910
	0.980	2.181	178.762	0.727	1.119	3.914	1.950
	1.960	2.216	181.631	0.739	1.128	4.025	1.965
	2.940	2.218	181.795	0.739	1.128	4.031	1.966

sample can easily be deformed at even lower loads, and the induced artificial cracks and dislocations can almost interact with each other, becoming nearly entangled.

That the fitting equations between F_{load} and H_v values also verifies the negative effect of Gd inclusions on the mechanical performance of the bulk Bi-2212 superconducting samples is the last finding for this part. The correspondence fitting parameters are numerically listed in Table 2. It is obvious from the table that the variation term of x^2 is found to be positive value of 0.0871 for the pure sample whereas the terms depending on x^2 are obtained to negative values in a range from −0.0349 to −0.1012 for the Ca-site Gd substituted Bi-2212 superconducting compounds. The former value of −0.0349 is attributed to the Gd-1 sample while the high value of −0.1012 is in association with the Gd-6 material. The differentiation of x^2 terms verifies the dramatic increment in the number of cracks, voids and dislocations through the consecutively stacked layers.

3.1.2 *Influence of Gd foreign impurities on mechanical characterization*

As for the variation of mechanical performance with the applied indentation test loads, two different characteristics appear: (I) standard indentation size effect (*ISE*) and (II)

Table 2 Microhardness fitting parameters based on the compression test load for every material

Materials	Fitting equations for pure and Ca/Gd substituted bulk Bi-2212 superconducting compounds
Gd-0	$\mathbf{y} = 0.0871\mathbf{x^2} - 0.3782\mathbf{x} + 4.4612$
Gd-1	$\mathbf{y} = -0.0349\mathbf{x^2} + 0.1511\mathbf{x} + 3.5637$
Gd-2	$\mathbf{y} = -0.0354\mathbf{x^2} + 0.1505\mathbf{x} + 3.3263$
Gd-3	$\mathbf{y} = -0.0503\mathbf{x^2} + 0.2129\mathbf{x} + 2.9721$
Gd-4	$\mathbf{y} = -0.0515\mathbf{x^2} + 0.2185\mathbf{x} + 2.5702$
Gd-5	$\mathbf{y} = -0.0775\mathbf{x^2} + 0.3252\mathbf{x} + 2.2967$
Gd-6	$\mathbf{y} = -0.1012\mathbf{x^2} + 0.4219\mathbf{x} + 1.8330$

unusual reverse indentation size effect (*RISE*) feature. The inner behavior displays the non-linear degradation of original microhardness characteristics (inverse dependence on indentation test load) with the increment of F_{load} while the latter feature shows the direct dependence on static test load applied [22–24]. Based on the figure, it is nature to confirm that the pure sample exhibits the non-linear microhardness feature known as the standard *ISE* behavior whereas the other Ca/Gd substituted Bi-2212 compounds present the unusual *RISE* feature. This is associated with the fact that the virgin material obtains both reversible (called as elastic) and irreversible (known as plastic) deformations while the plastic deformation becomes more and more dominant with the presence of Gd impurities inserted in the Bi-2212 crystal system. Thus, it is necessary to underline that the Gd nanoparticles lead to disappear of the elastic recovery belonging to the Bi-2212 inorganic solid material [25–27]. It is another probable result deduced from this study that the *RISE* behavior of mechanical characteristics tends to improve regularly with the increase of Gd inclusions in the crystal structure due to the augmented local structural distortions, disorders in orientation of consecutively stacked plates, lattice strains, defects and grain boundary couplings. This fact is even favored by the significant decrease in the Vickers hardness parameters up to the critical static test load value of about 2 N beyond which (load independent region) the parameters remain constantly. Figure 1 guarantees that the Gd-6 material reaches more rapidly to its saturation limit value than the pure and other Ca/Gd partially substituted Bi-2212 materials.

The combination of the results inferred from last two sections declares that the existence of Gd inclusions in the Bi-2212 crystal matrix leads to induce new crack-producing omnipresent flaws (the stress raisers and crack initiation sites). Hence, the propagation of flaws, dislocation movements and crack accelerates throughout the entire bulk materials due to the reduction of Griffith critical crack length, and the mechanical performance (durability, stiffness, fracture and flexural strengths) and characteristics (*ISE* or *RISE* nature) diminish drastically, the critical stress value and durable tetragonal phase as they do.

3.1.3 *Determination of load dependent characteristic parameters*

In this part of the present study, by using the following equations we deduce the crucial mechanical characteristics as regards the yield strength, elastic modulus (E), brittleness index (B), fracture toughness (K_{IC}) and elastic stiffness coefficient (C_{11}) parameters, which are responsible for the usage in the technological, engineering and industrial applications of the Bi-2212 ceramic compounds.

$$E = 81.9635H_V \tag{2}$$

$$Y \approx \frac{H_V}{3} \tag{3}$$

$$K_{IC} = \sqrt{2E\alpha} \quad (\alpha,\ \text{surface energy}) \tag{4}$$

$$B = \frac{H_v}{K_{IC}} \tag{5}$$

$$C_{11} = H_v^{7/4} \tag{6}$$

Every calculation is embedded in Table 1. It is visible from the table that both the Gd content level and applied test loads affect strongly the computations. Firstly, we focus on the elastic modulus parameters of the Bi-2212 superconducting materials. The elastic moduli degrade considerably with the increasement in the Gd impurities. At the static test load of 0.245 N, the maximum and minimum elastic modulus parameters are found to be about 362 and 152 GPa for the pure and Gd-6 bulk samples, respectively. This corroborates that the presence of highest Gd concentration level damages considerably the mechanical stability, stiffness, durability, fracture and flexural strength of the Bi-2212 crystal structure. The long and short of it is that the increase in the Gd addition degrades the resistant towards to the permanent plastic deformation or strain. As for the change of elastic moduli with the applied static test loads, the Young's moduli of Gd-0 bulk material tend to decrease with the applied indentation test loads; on the other hand, the modulus values belonging to the Ca/Gd substituted Bi-2212 superconducting ceramics increase continuously with the enhancement in the static test load

applied. This differentiation stems from the mechanical characterization of the materials prepared in this work. Namely, the pure sample presents the standard *ISE* behavior whereas the other materials (Ca/Gd partial replaced Bi-2212 inorganic compounds) exhibit the unusual *RISE* feature. In other words, the Gd additives make both the mechanical characteristics and surface energy values of the Bi-2212 matrix change harshly.

At the same time, we are interested in the beginning point of permanent plastic deformation with the Gd foreign impurities inserted in the Bi-2212 crystal structure. According to Table 1, the yield strength parameters tend to decrease with the enhancement of the Gd concentration level in the Bi-2212 crystal core. In this respect, the maximum yield strength value of 1.47 GPa is observed for the Gd-0 material while the lowest value of 0.62 GPa is attributed to the bulk Gd-6 compound at the constant compressive load of 0.245 N. This is in accordance to the increase of induced artificial voids and cracks in the Bi-2212 crystal lattice with the Gd additives. Accordingly, the beginning point of permanent plastic deformation for the poly-crystallized Bi-2212 material considerably shifts to the lower load values. Moreover, we deal with the test load effect on the yield strength parameters of the pure and Ca/Gd substituted Bi-2212 ceramics. It is visible from Table 1 that the yield strength values belonging to the Gd-0 sample decrease monotonously from 1.47 to 1.36 GPa with ascending static compression loads in the range of 0.245–2.940 N. In contrast, the beginning points of permanent plastic deformation for the Ca/Gd substituted Bi-2212 materials increase systematically with the applied load. This is consistent with the fact that the presence of Gd inclusions in the Bi-2212 system changes the mechanical characteristics from the typical *ISE* nature to *RISE* behavior.

Additionally, we examine the resistance against the beginning of permanent distortion or strain of the pure and Ca-site Gd substituted Bi-2212 ceramics. Every fracture toughness parameter is deduced from Eq. (4) and numerically gathered in Table 1. It is seen from the table that the highest values of fracture toughness parameter are observed for the Gd-free Bi-2212 sample at each static test load. This means that the distortion or strain energy generated from disordered crystal lattices of the Gd-0 sample is at the minimum level as compared to those of the other materials. Hence, the propagation of induced cracks and dislocation movements in the pure compound is more easily controlled due to the higher critical stress value. In other words, the movement of induced cracks, voids and dislocations in the Ca/Gd substituted materials reaches rapidly to their critical propagation speed values as a result of decrease in the Griffith critical crack length. The propagation of induced cracks and dislocation movements is accordingly difficult to control.

We also investigate the variation of resistant against the permanent plastic deformation or strain with the Gd addition in the Bi-2212 crystal. In this regard, the elastic stiffness coefficients are determined by using Eq. (6). All the calculations are numerically tabulated in Table 1 in detail. According to the table, the Gd-0 material obtains the maximum elastic stiffness coefficients at each applied test load whereas the Gd-6 compound has the global minimum coefficient values. In fact the elastic stiffness coefficient is calculated to be 13.46 GPa (maximum value) for the pure sample whereas the minimum value of 2.95 GPa is attributed to the Gd-6 material under the static applied test load of 0.245 N. It is reasonable to conclude that the mechanical strength (durability and stiffness), fracture and flexural strengths (related to resistant towards permanent plastic deformation or strain) of the Bi-2212 texturing diminish extensively. Therefore, the propagations proceed throughout the intergranular regions (grain boundaries) instead of transgranular regions (in the grains), and the material is more easily broken. Besides, one can encounter the changes in the bond strengths of $Cu–O_2$ consecutively stacked sheets (Table 1).

3.1.4 *Load independent microhardness parameters based on Hays–Kendall approach*

Although there are many theoretical models for the mechanical identification and performance in the literature, we prefer only Hays–Kendall (*HK*) approach. As well known, generally the theoretical model is found to be the best approach for the superconducting materials [28]. *HK* model proposed by Hays and Kendall [29] exhibits perfectly approaches on the mechanical performance and characterization belonging to the bulk Bi-2212 materials. Throughout the computations, the permanent plastic deformation begins to play the predominant role after the certain test load value of W and thus the elastic recovery disappears immediately. In this respect, the indenter penetrates intensely into the bulk material at the higher indentation test load of W [30], and the length of indentation notch is determined from the effective load value of $F_{eff} = F - W_{HK}$ by the following equation:

$$F - W = A_{HK} d^2 \tag{7}$$

where the constant of A_{HK} presents the microhardness parameter, and the value of W constant denotes the applied static test load. For the materials the linear graphics related to F over d^2 are depicted in Fig. 2. With the aid of the extrapolation methods, the parameters of A_{HK} and W inferred from the graphics are numerically listed in Table 3. It is visible from the table that only the pure Bi-2212 sample obtains the positive W number whereas the Ca/Gd substituted Bi-2212 materials have the negative W

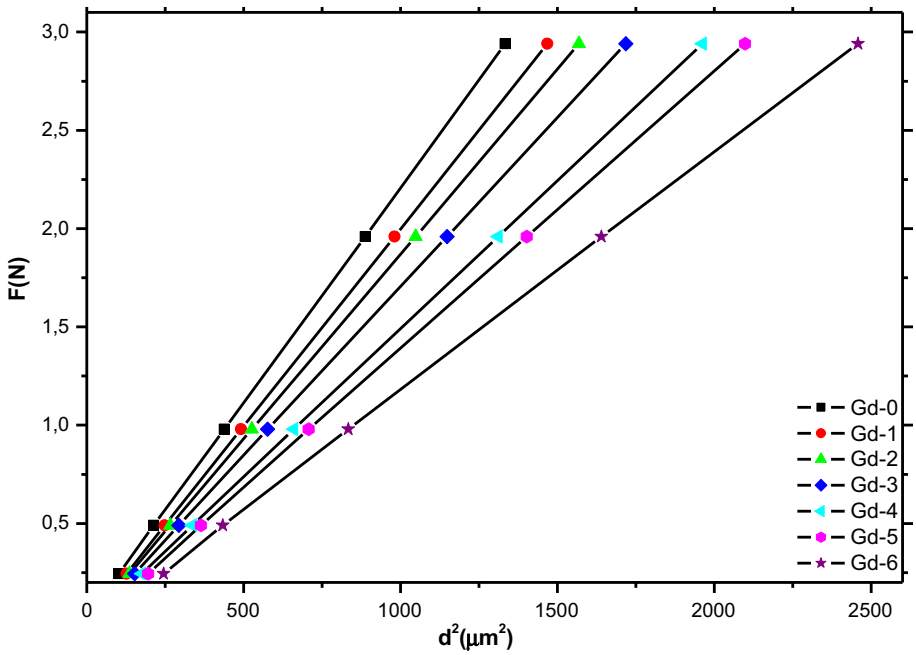

Fig. 2 Linear plots of indentation test load F over indentation impression length d^2 of the pristine and Ca-site Gd substituted ceramics

Table 3 Extrapolated A_{HK} and W constants evaluated from Hays–Kendall approach and original Vickers hardness parameters of H_v and H_{HK} in the saturation limit regions

Samples	Hays–Kendall approach results			
	W (N)	$A_{HK} \times 10^{-3}$ (N/μm^2)	H_{HK} (GPa)	H_V (GPa)
Gd-0	0.0207	0.219	4.061	4.094–4.089
Gd-1	−0.0098	0.201	3.727	3.703–3.714
Gd-2	−0.0106	0.188	3.486	3.467–3.476
Gd-3	−0.0146	0.172	3.190	3.166–3.174
Gd-4	−0.0175	0.151	2.800	2.771–2.778
Gd-5	−0.0267	0.142	2.633	2.592–2.598
Gd-6	−0.0409	0.122	2.262	2.216–2.218

number. This is attributed to the fact that the former material exhibits the typical *ISE* feature; on the other hand, the other materials present the unusual *RISE* behavior. In this regard, under the test load applied the plastic (irreversible) deformation is encountered to be the predominant character in the presence of the Gd inclusions, and thus the elastic recovery disappears immediately in the Bi-2212 crystal matrix. In fact, the W parameter tends to decrease regularly with the increment in the Gd concentration level. It is tempting to speculate that the local structural distortions, lattice strains/defects/disorders and grain boundary coupling problems increase with the Gd impurities in the adjacent layers. At the same time, the variation of A_{HK} constants with the dopant level is another probable result deduced from the *HK* model. According to Table 3, the A_{HK} parameter values degrade constantly with the increase of the Gd content level in the Bi-2212 crystal lattice. The practical consequence evaluated from the theoretical method is that the Gd decorations damage significantly the mechanical strength (durability and stiffness), fracture and flexural strength properties of the Bi-2212 crystal structure. The findings of *HK* approach declare that the Gd inclusions retrograde the critical stress and durable tetragonal phase. Similarly, the increase artificial cracks, voids and dislocation movements reach rapidly to their critical propagation speeds as a consequence of the decrement in Griffith critical crack length, and thus the intergranular fracture becomes more dominant in the Bi-2212 matrix. Furthermore, we extract the real (load independent) Vickers hardness parameters in the plateau limit values obtained from Fig. 1 with the use of the following relation:

$$H_{HK} = 1854.4A_{HK} \quad (8)$$

Every computed H_{HK} constants are numerically provided in Table 3. It is seen that all the theoretical calculations are found to be much closer (slight smaller) to the load independent Vickers hardness parameters in the plateau regions. Hence, the *HK* theoretical approach is reliable and

suitable model to discuss the mechanical performances and characterizations of pure and Ca/Gd substituted Bi-2212 materials. All in all, the modelling of Vickers hardness parameters enables the researchers to describe the crucial changes in the mechanical properties belonging to the Bi-2212 materials exposed to the Gd impurities.

4 Conclusion

In the present study, we examine the crucial changes in the mechanical performance and characterization of the Bi-2212 ceramic materials exposed to the Ca/Gd substitution by use of the microhardness measurements conducted at indentation test loads ($0.245 \leq F_{load} \leq 2.940$ N). Besides, we evaluate the role of Gd foreign impurities on the propagation of artificial cracks, voids and dislocation movements. Likewise, we determine the differentiation of the critical propagation speeds, Griffith critical lengths, critical stress values and durable tetragonal phases with the Gd decorations. At the same time, the load dependent mechanical characteristics including Young's moduli, yield strengths, fracture toughness, brittleness indices and stiffness coefficients, being responsible for the usage in metallurgical, engineering, industrial, technological and large scale applications of the materials, are sensitively deduced from the microhardness curves. All the experimental and extracted findings show that the existence of Gd nanoparticles in the Bi-2212 system leads to damage the local structural distortions, grain boundary couplings and lattice disorders/strains/defects in the orientation of consecutively stacked layers. Moreover, we discuss the variation of mechanical properties by means of the Hays–Kendall approach for the first time. Similarly, the reliability and suitability of the theoretical model preferred are also explored in the saturation limit (load independent) regions. The major evidences inferred from this work are the followings:

- The mechanical performance suppresses constantly with the increase of Gd foreign impurities inserted in the Bi-2212 crystal lattice due to the augmentation in the local structural distortions, lattice strains/defects and grain boundary coupling problems in the Cu–O_2 consecutively stacked sheets. Thus, the critical stress value, Griffith critical crack length and durable tetragonal phase reduce considerably. The differentiations are also verified by the fitting equations between F_{load} and H_v values.
- Similarly, the Gd additives cause to induce the crack-producing omnipresent flaws serving as the stress raisers and crack initiation sites. Accordingly, the propagation of induced artificial cracks, voids and dislocation movements reaches hastily to the critical speed value, and the intergranular fracture plays more dominant role in the Bi-2212 matrix. Hence, the bulk material is broken easily. The long and short of it is that the Gd nanoparticles are ploughed to improve the mechanical performance as regards the mechanical strength (durability and stiffness), fracture and flexural strengths of the Bi-2212 material due to the augmented operable slip systems.
- The Vickers hardness curves obtained display that the virgin material shows the typical *ISE* feature while the Ca/Gd substituted Bi-2212 compounds exhibit the unusual *RISE* feature. This is in relation to the fact that the irreversible deformations in the Bi-2212 crystal system become more and more dominant with increasing Gd impurities. Thus, the elastic recovery disappears immediately for the Ca-site Gd substituted bulk Bi-2212 materials. Moreover, the increase of Gd concentration level in the Bi-2212 system favors continuously the *RISE* behavior.
- The extracted parameters such as Young's modulus, yield strength, brittleness index and elastic stiffness coefficient indicate that the presence of Gd nanoparticles in the crystal lattice damages considerably the mechanical stability, stiffness, durability, fracture and flexural strength of the Bi-2212 material. Accordingly, crystal structure needs less required energy to propagate induced cracks, voids and dislocation movements and to reach them to the critical propagation speed.
- The theoretical modelling demonstrates that the *HK* approach is adequate descriptor to define mechanical characteristics (standard *ISE* or unusual *RISE* behavior) of the virgin and Ca/Gd substituted Bi-2212 ceramic samples. Besides, the *HK* model succeeds to show the improvement of the *RISE* feature with the enhancement in the Gd foreign inclusions in the crystal structure. At the same time, the *HK* approach is found to be valid model for discussion of the load independent Vickers hardness parameters in the plateau regions.
- To sum up, the Gd additives behaving as crack-producing omnipresent flaws (the stress raisers and crack initiation sites) give rise to damage the mechanical durability, stiffness, fracture and flexural strength properties. Thus, the substitution of Gd nanoparticle at the Ca site in the Bi-2212 crystal system is not a suitable method to improve mechanical performance and characterization of the Bi-2212 material and to use the compounds in the metallurgical, engineering, technological and industrial applications.

Acknowledgments This study is partially supported by Abant Izzet Baysal University Scientific Research Project Coordination Unit (Project No: 2014.09.05.685).

References

1. R. Chattopadhyay, *Surface Wear: Analysis, Treatment, and Prevention*, 1st edn. (ASM International Publishers, OH, 2001)
2. F. Wredenberg, P.L. Larsson, Scratch testing of metals and polymers: experiments and numerics. Wear **266**, 76–83 (2009)
3. H.W. Zhao, Y.X. Zhong, Z.C. Ma, J. Alloys Compd. **680**, 105–108 (2016)
4. M. Dogruer, C. Terzioglu, G. Yildirim, O. Gorur, J. Supercond. Nov. Magn. **27**, 755–761 (2014)
5. H. Koralay, O. Hicyilmaz, S. Cavdar, E. Asikuzun, A.T. Tasci, O. Ozturk, J. Mater. Sci. Mater. El. **25**, 3116–3126 (2014)
6. E. Akdemir, M. Pakdil, H. Bilge, M.F. Kahraman, G. Yildirim, E. Bekiroglu, Y. Zalaoglu, E. Doruk, M. Oz, J. Mater. Sci. Mater. El. **27**, 2276–2287 (2016)
7. R. Awad, A.I. Abou-Aly, M.M.H. Abdel, Gawad, I. G-Eldeen. J. Supercond. Nov. Magn. **25**, 739–745 (2012)
8. N.K. Saritekin, Y. Zalaoglu, G. Yildirim, M. Doğruer, C. Terzioglu, A. Varilci, O. Gorur, J. Alloys Compd. **610**, 361–371 (2014)
9. M. Dogruer, C. Terzioglu, G. Yildirim, M. Pakdil, Y. Zalaoglu, J. Mater. Sci. Mater. El. **26**, 6013–6019 (2015)
10. G. Murugesan, S. Kalainathan, J. Alloys Compd. **677**, 121–126 (2016)
11. S.M. Walley, Historical origins of indentation hardness testing. Mater. Sci. Technol. **28**, 1028–1044 (2012)
12. F. Tancret, I. Monot, F. Osterstock, Mat. Sci. Eng. A Struct. **298**, 268–283 (2001)
13. N.K. Saritekin, C. Terzioglu, M. Pakdil, T. Turgay, G. Yildirim, J. Mater. Sci. Mater. Electron. **27**, 1854–1865 (2015)
14. P.P. Bhattacharjee, R.K. Ray, A. Upadhyaya, Mat. Sci. Eng. A Struct. **488**, 84–91 (2008)
15. F. Kahraman, J. Mater. Sci. Mater. El. (2016). doi:10.1007/s10854-016-4796-7
16. J. Gong, J. Wu, Z. Guan, J. Eur. Ceram. Soc. **19**, 2625–2631 (1999)
17. A.A. Elmustafa, D.S. Stone, J. Mech. Phys. Solid **5**, 357–381 (2003)
18. K. Sangwal, Mater. Chem. Phys. **63**, 145–152 (2000)
19. R. Awad, A.I. Abou-Aly, M. Kamal, M. Anas, J. Supercond. Nov. Magn. **24**, 1947–1956 (2011)
20. Y. Zalaoglu, E. Bekiroglu, M. Dogruer, G. Yildirim, O. Ozturk, C. Terzioglu, J. Mater. Sci. Mater. El. **24**, 2339–2345 (2013)
21. T.P. Sheahen, *Introduction to High-Temperature Superconductivity*, 1st edn. (Kluwer Academic Publishers, New York, 2002)
22. F. Poehl, S. Huth, W. Theisen, Int. J. Solids Struct. **84**, 160–166 (2016)
23. M.M. Pasare, M.I. Petrescu, Mater. Plast. **45**, 87–90 (2008)
24. R.K.A. Al-Rub, Mech. Mater. **39**, 787–802 (2007)
25. H. Li, R.C. Bradt, J. Mater. Sci. **31**, 1065–1070 (1996)
26. F. Fröhlich, P. Grau, W. Grellmann, Phys. Stat. Solidi A **42**, 79–89 (1977)
27. W.C. Oliver, R. Hutchings, J.B. Pethica, in *Microindentation Techniques in Materials Science and Engineering*, ed. by P.J. Blau, B.R. Lawn (ASTM STP 889, Philadelphia, 1986)
28. M. Dogruer, F. Karaboga, G. Yildirim, C. Terzioglu, O. Ozturk, J. Mater. Sci. Mater. El. **24**, 2659–2666 (2013)
29. C. Hays, E.G. Kendall, Metallography **6**, 275–282 (1973)
30. M.B. Turkoz, S. Nezir, O. Ozturk, E. Asikuzun, G. Yildirim, C. Terzioglu, A. Varilci, J. Mater. Sci. Mater. El. **24**, 2414–2421 (2013)